



## A circular cross-section PDMS microfluidics system for replication of cardiovascular flow conditions

Lindsey K. Fiddes<sup>a</sup>, Neta Raz<sup>a</sup>, Suthan Sriganapalan<sup>b,c</sup>, Ethan Tumarkan<sup>a</sup>, Craig A. Simmons<sup>b,c</sup>, Aaron R. Wheeler<sup>a,b,\*\*</sup>, Eugenia Kumacheva<sup>a,\*</sup>

<sup>a</sup> Department of Chemistry, University of Toronto, 80 St. George Street, Toronto, Ontario M5S 3H6, Canada

<sup>b</sup> Institute of Biomaterials and Biomedical Engineering, University of Toronto, 164 College Street, Toronto, Ontario M5S 3G9 Canada

<sup>c</sup> Department of Mechanical and Industrial Engineering, University of Toronto, 5 King's College Road, Toronto, Ontario M5S 3G8, Canada

### ARTICLE INFO

#### Article history:

Received 29 November 2009

Accepted 13 January 2010

Available online 18 February 2010

#### Keywords:

Microchannels

Flow

Cardiovascular system

Circular cross-section

Patterning

Seeding of endothelial cells

### ABSTRACT

Since the inception of soft lithography, microfluidic devices for cardiovascular research have been fabricated easily and cost-effectively using the soft lithography method. The drawback of this method was the fabrication of microchannels with rectangular cross-sections, which did not replicate the circular cross-sections of blood vessels. This article presents a novel, straightforward approach for the fabrication of microchannels with circular cross-sections in poly(dimethylsiloxane) (PDMS), using soft lithography. The method exploits the polymerization of the liquid silicone oligomer around a gas stream when both of them are coaxially introduced in the microchannel with a rectangular cross-section. We demonstrate (i) the ability to control the diameter of circular cross-sections of microchannels from ca. 40–100  $\mu\text{m}$ ; (ii) the fabrication of microchannels with constrictions, and (iii) the capability to grow endothelial cells on the inner surface of the microchannels.

© 2010 Elsevier Ltd. All rights reserved.

### 1. Introduction

In the past decade, microfluidics has emerged as a powerful tool for mimicking cardiovascular systems. Microchannels with varying geometries and surface properties have been used to study the behavior of individual cells and cell suspensions under dynamic conditions [1–7]. For example, in studies of flow of individual cells in glass capillaries coated with small molecules or proteins it has been established that cell attachment to the capillary wall enhances with decreasing shear stress [2]. By constructing a flow profile of red blood cells in a glass capillary it was established that the resistance to flow can significantly increase when a single neutrophil blocks the channel [8]. In another series of experiments conducted for blood with 20% haematocrit in microchannels with a rectangular cross-section, good agreement was found between experimental and theoretical velocity profiles in the middle plane of the channel, whereas noticeable deviations between theory and experiments existed at locations close to the channel walls [9].

Since the inception of soft lithography, microfluidic research on cardiovascular systems has been dominated by studies conducted in microfluidic devices fabricated in polydimethylsiloxane (PDMS) [1,3–7,9–11]. PDMS devices are cost-efficient, oxygen-permeable and non-cytotoxic. Furthermore, the ability to replicate complex geometries of the micro-cardiovascular system and to precisely tune the dimensions of microchannels have made the soft lithography method very beneficial for cell studies [6]. Yet, the drawback of PDMS devices produced by this method is the rectangular cross-section of microchannels [12], which does not replicate the circular cross-section of blood vessels. Under constrained conditions, that is, when cell dimensions are larger than the diameter of a blood vessel [8], cells act as plugs: they experience a shear stress, elongate, and due to the pressure build-up, are pushed through the constriction [6,8]. In microchannels with a rectangular cross-section spherical cells do not conformally plug a microchannel. The flow of the continuous liquid phase occurs through four corners of the microchannel, thereby changing the shear stress imposed on the cell and influencing the pressure build-up in the channel. Furthermore, in rectangular channels the area of contact of confined cells with the microchannel walls is reduced, and the flow profile of the cells differs from that in a channel with a circular cross-section [13,14]. These features preclude accurate mimicking of the flow of cells through the blood capillaries by using the microchannels fabricated by soft lithography.

\* Corresponding author. Tel./fax: +1 416 978 3576.

\*\* Corresponding author. Department of Chemistry, University of Toronto, 80 St. George Street, Toronto, Ontario M5S 3H6, Canada. Tel.: +1 416 946 3864; fax: +1 416 946 3865.

E-mail addresses: [awheeler@chem.utoronto.ca](mailto:awheeler@chem.utoronto.ca) (E. Wheeler), [ekumacheva@chem.utoronto.ca](mailto:ekumacheva@chem.utoronto.ca) (E. Kumacheva).

Microchannels with a circular cross-section were fabricated by casting PDMS around templates such as glass capillaries [10], stainless steel rods [15–17], and nylon threads [18]. The main detriment of these methods for studies of cells in constrained geometries is an insufficient ability to gradually change the diameter of the microchannel. Moreover, with rigid templates fabrication of channels with complex geometries and especially, channel networks becomes a challenge. A useful method includes fabrication of PDMS channels with a rectangular cross-section, followed by its subsequent transformation to a circular one [19,20]. Reshaping rectangular cross-sections using silica sol gel reactions [16], polymerization of low molecular weight silicone oligomers [20,21], or modification of SU8 masters [22] was used for the preparation of microchannels with circular cross-sections; however, these works lack the control to gradually change the diameter of microchannels, which is critically important for studies of cells under confinement.

Here we describe a simple, straightforward approach to producing microchannels with a circular cross-section in microfluidic devices fabricated in PDMS. Our strategy includes (i) the fabrication of microchannels with a rectangular cross-section using a soft lithography method; (ii) the introduction in the microchannel of a coaxial stream of a gas and a solution of the silicone oligomer in an organic solvent; (iii) the polymerization of the oligomer around the gas stream and the removal of the solvent. In our strategy, the gas stream serves as a template that controls the shape and the diameter of the cross-section of the fabricated microchannel. Furthermore, we show the ability to seed a monolayer of endothelial cells on the surface of circular channels. The proposed method can be successfully used for the fabrication of microchannels with varying diameters, which can be used for optical microscopy studies of flow of “surrogate” cells under constrained conditions [23,24].

## 2. Experimental design

### 2.1. Fabrication of PDMS microchannels

Microfluidic channels were fabricated in PDMS (Sylgard 184 Silicone Elastomer Kit, Dow Corning Corp., Midland, MI) using a standard soft lithography method [12]. Fluidic ports were fabricated using a cork borer to make a 17 gauge inlet. A patterned PDMS sheet was sealed to a planar PDMS sheet using plasma-induced bonding (550 mTorr in air, 90 s) and the device was subsequently incubated in air at 72 °C to render the surface of PDMS hydrophobic.

The devices were examined using an optical microscope (Olympus BX51) equipped with a camera (Olympus U-CAMD3). The images were analyzed using Image Pro Plus software (Media Cybernetics, MD, USA). We examined the modification of microchannels with three designs. First, we modified a rectangular cross-section of microchannels with dimensions  $100\ \mu\text{m} \times 115\ \mu\text{m} \times 5\ \text{cm}$ . The second set of microchannels with dimensions  $100\ \mu\text{m} \times 115\ \mu\text{m} \times 5\ \text{cm}$  was topographically patterned with  $300\ \mu\text{m} \times 60\ \mu\text{m}$  constrictions, which were separated by the distance 2 mm. A third set of microchannels was used for cell growth and had the dimensions  $1\ \text{mm} \times 1\ \text{mm} \times 5\ \text{cm}$ .

#### 2.1.1. Modification of rectangular PDMS microchannels

Fig. 1 shows the schematics of the proposed approach. A microchannel with a square cross-section is fabricated in PDMS by the soft lithography method (Fig. 1A). Using a syringe with an 18 gauge needle and 17 gauge o.d. teflon tubing (Small Parts, USA), the channel is manually filled with a solution of silicone oligomer prepared by dissolving the silicone oligomer and the initiator (in a 10 to 1 ratio) in hexanes (Sigma–Aldrich Canada) at different concentrations (Fig. 1B). In the next step, a stream of  $\text{N}_2$  from a tank is introduced in the channel via Teflon tubing. The tubing is sealed to the device with an epoxy resin (LePage, Canada). The  $\text{N}_2$  pressure was varied using a pressure gauge (Bellofram Corp., USA). The  $\text{N}_2$  stream forms a gaseous thread with a circular cross-section in the center of the channel (Fig. 1C). The device is placed for 10 min on a hot plate at 100 °C. The polymerization of the silicone oligomer around the  $\text{N}_2$  stream, and the evaporation of the hexanes leave behind a circular microchannel (Fig. 1D). In the described approach, the stream of  $\text{N}_2$  acts as a fluid template determining the dimensions of the circular microchannel. Once the silicone oligomer is polymerized, the passage of  $\text{N}_2$  is terminated, the microfluidic device is cooled to room temperature and is ready for use.

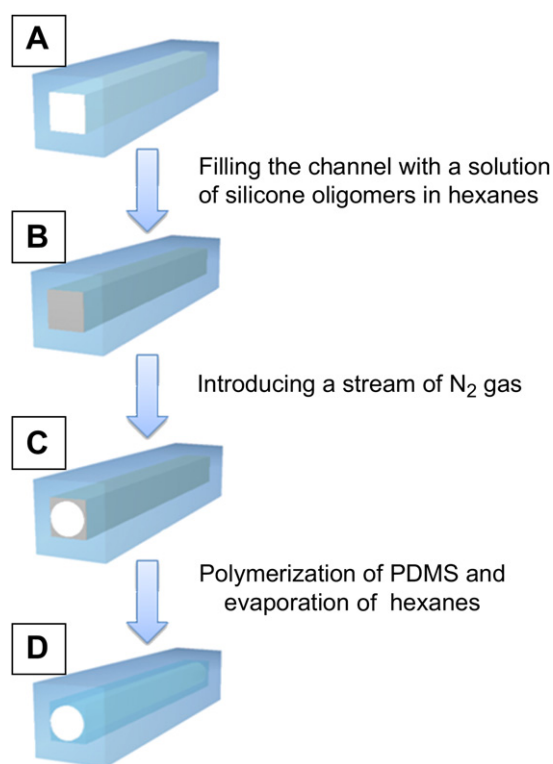


**Fig. 1.** Schematic of the fabrication of microchannels with circular cross-sections. (A) Original microchannel with square cross-section fabricated by the soft lithography method; (B) Microchannel filled in with a solution of silicone oligomer in hexanes (grey color); (C) Microchannel as in (B) with a stream of  $\text{N}_2$  (white color) passing along the channel; (D) Microchannel with a circular cross-section following polymerization of silicone oligomers.

In the present work, we examined the effect of pressure,  $P_{\text{N}_2}$ , of the nitrogen gas, and concentration,  $C_{\text{B}}$ , of the silicone oligomer in the hexane mixture, on the microchannel diameter,  $D_{\text{m}}$ . Each experiment was run using 5 devices. To measure the value of  $D_{\text{m}}$ , the devices were cut at positions 1, 2.5 and 4 cm from the inlet, and the diameter of the microchannel cross-section was examined by optical microscopy. The variation in the value of  $D_{\text{m}}$  originated from the difference in microchannel diameter in different microfluidic devices, as well as the variation in the diameter of the microchannel in three aforementioned positions. Along the channel, the variation in  $D_{\text{m}}$  did not exceed several micrometers.

#### 2.1.2. Modification of rectangular microchannels with a constriction

The method illustrated in Fig. 1 was also used to modify the cross-section of microchannels with a  $300\ \mu\text{m} \times 60\ \mu\text{m}$  constriction located 2.5 cm from the inlet of the microchannels. The rectangular cross-section of the constriction was transformed into a circular one by polymerizing silicone oligomers in a 50 wt.% solution in hexanes around the  $\text{N}_2$  stream at a pressure of 15 psi. To measure the diameter of the circular microchannel in the constriction, a 5 mg/mL aqueous solution of a fluorescent dye Rhodamine B was introduced into the microchannel and fluorescence images of the channels were acquired immediately after the solution and analyzed.

#### 2.1.3. Patterning circular microchannels with endothelial cells

The method illustrated in Fig. 1 was used to modify microchannels with the dimensions  $1\ \text{mm} \times 1\ \text{mm} \times 5\ \text{cm}$ . The microchannels were filled with 90 wt.% PDMS in hexanes and flashed with  $\text{N}_2$  at pressure of 5 psi. After polymerizing PDMS on a hot plate for 10 min, the devices were placed in a 140 °C oven for 2 h to ensure complete evaporation of hexanes. Once the device cooled to room temperature, tetraethyl orthosilicate was injected into the channels and the device was returned to the 140 °C oven for 0.5 h to form a thin  $\text{SiO}_2$  layer on the surface of PDMS [22]. The  $\text{SiO}_2$  layer aided in cell adhesion to the channel walls. Once the device was cooled to room temperature, an aqueous solution of 1 mg/mL fibronectin (Sigma–Aldrich, Oakville, ON) was injected into the channels for 2 h to adsorb to the channel surface. Primary porcine aortic endothelial cells (PAECs) were injected into the channels at the concentration of  $1 \times 10^6$  cells/mL and were cultured in M199 (Sigma) supplemented with 5% fetal bovine serum (Fisher Scientific, Ottawa, ON), 5% cosmic calf serum (Fisher Scientific), and 1% penicillin–streptomycin. The microchannels were

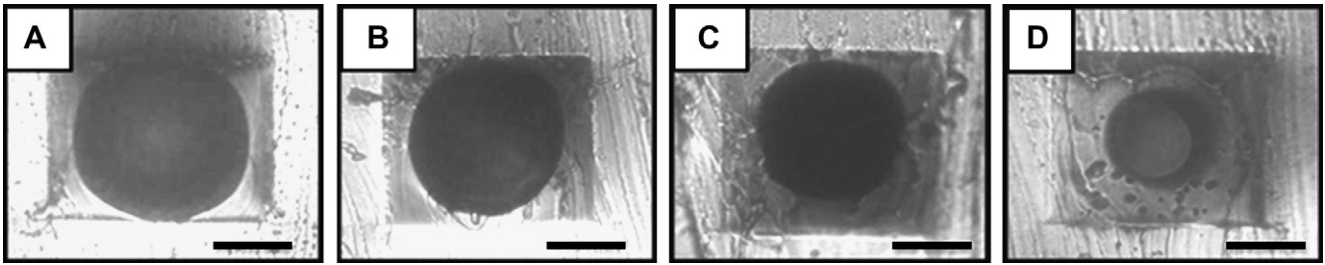


**Fig. 2.** (A–D) Bright field images of the cross-sectional area of the microchannels produced at  $C_{\text{PDMS}} = 50\%$  at  $P_{\text{N}_2}$  of 15 psi (A), 12.5 psi (B), 10 psi (C), and 5 psi (D). Scale bar is 40  $\mu\text{m}$ .

placed into an incubator for 10 min to allow cells time to settle. The devices were then reseeded with cells [25], rotated by 90° and again placed into an incubator for 10 min. This step was repeated two more times to cover the entire surface of the circular channels with cells. During the reseeding processes a flow rate of less than 0.1 mL/h is used to keep shear stresses in the channel minimal to avoid cell detachment from the walls. After the last cell suspension was injected, the microchannels were placed upright into an incubator for 4 h. After this time interval, 500  $\mu\text{L}$  of culture media was injected into each channel to feed attached cells, and remove any unbound cells. After 24 h, PAECs were fixed within microchannels using 10% neutral buffered formalin and permeabilized with 0.1% Triton X-100 (Fisher Scientific). Cells were stained for filamentous (F)-actin and nuclei using fluorescein isothiocyanate (FITC)-conjugated phalloidin (1:100 dilution) (Sigma) and Hoechst (1:1000 dilution) (Invitrogen, Burlington ON), respectively.

### 3. Results and discussion

#### 3.1. Variation of microchannel diameter with varying nitrogen pressure

Fig. 2 shows bright field optical microscopy images of the transformation of the rectangular microchannel cross-section into a circular one, achieved at  $C_p = 50\text{ wt.}\%$  and  $\text{N}_2$  pressure varying from 5 to 15 psi. With two-phase flow, the diameter in the inner phase has been shown to increase with increasing pressure of the inner phase [26]. For the  $\text{N}_2$  gas pressure in the range  $5 < P_{\text{N}_2} < 15$  psi the microchannels had circular cross-sections with well-defined, controllable diameters, and the circular ‘opening’ was symmetric, with the ratio of the vertical to horizontal diameters of  $1 \pm 0.05$ . With decreasing value of  $P_{\text{N}_2}$  the diameter of the circular channel reduced. For  $P_{\text{N}_2} > 15$  psi, the microchannel had a square cross-section with rounded corners, whereas microchannels generated at  $P_{\text{N}_2} < 5$  psi had circular cross-sections with varying diameters. The latter effect occurred due to Rayleigh-Plateau hydrodynamic instabilities in the  $\text{N}_2$  gas stream, so that small perturbations in the stream were replicated in silicone oligomer polymerized around the stream.

Fig. 3 shows the variation in the diameter of the circular microchannel and the corresponding change in the cross-sectional area of the microchannel, both plotted as a function of the pressure of  $\text{N}_2$ . With decreasing  $P_{\text{N}_2}$  the diameter of the channel gradually reduced, and the smallest diameter of 39  $\mu\text{m}$  was obtained at  $P_{\text{N}_2} = 5$  psi. The variation in the cross-sectional area of the microchannel, characterized as the ratio,  $S/S_0$ , between the cross-sectional areas of the circular microchannel and the original square microchannel, respectively, is shown in Fig. 3B. With increasing  $P_{\text{N}_2}$ , the cross-sectional area of the circular microchannels featured a linear increase.

#### 3.2. Variation in microchannel diameter with varying concentration of silicone oligomer

In the next step, we examined the effect of the concentration of silicone oligomer in the solution in hexanes on the variation of the diameter of circular microchannel. Fig. 4A shows that as  $C_p$

increased from 10 to 50 wt.%, the diameter of the circular cross-section of the microchannel decreased from 100 to 39  $\mu\text{m}$ . The cross-sectional area of the microchannel showed a linear decrease with increasing concentration of silicone oligomers (Fig. 4B).

Using  $C < 10\text{ wt.}\%$  did not allow the transformation of rectangular channels into the circular ones: the cross-section had a rounded square shape. For  $C_p > 50\text{ wt.}\%$  the solution of silicone oligomer in hexanes had high viscosity and the circular channels had a varying value of  $D_m$ . This effect occurred due to the distribution of velocities of the liquid across the channel: the velocity of the fluid was the greatest at the center of the microchannel and exponentially decreased towards zero at the side wall where a layer of static fluid existed. In a binary fluid system used in our work, a higher viscosity of the outer liquid phase led to the increased thickness of the static layer, since the velocity profile of the inner phase experienced a steeper exponential decay close to the side wall of the channel.

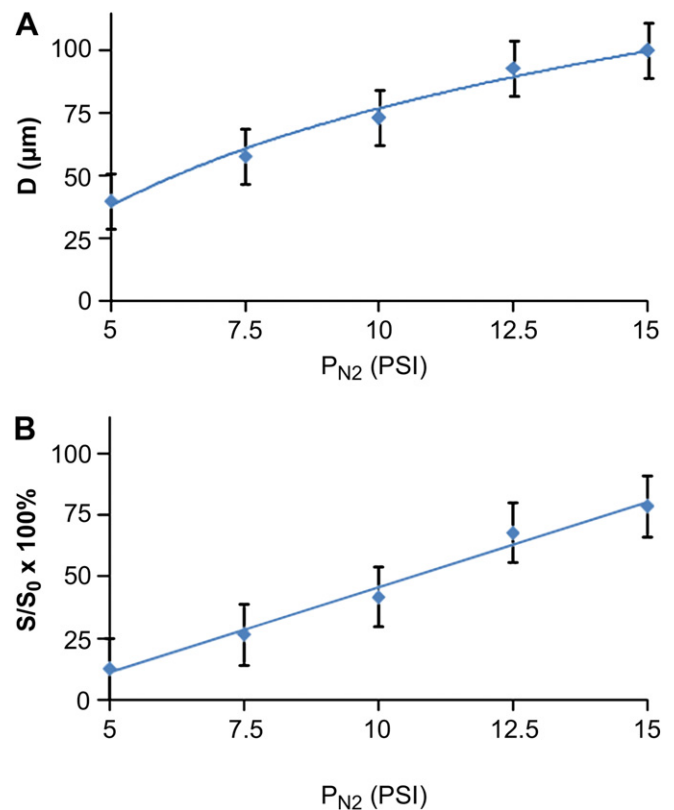


**Fig. 3.** Variation in the diameter,  $D_m$ , of the circular channel (A) and the respective cross-sectional area ( $S/S_0$ ) of the circular channel (B), both plotted as a function of nitrogen pressure  $C_p = 50\text{ wt.}\%$ .

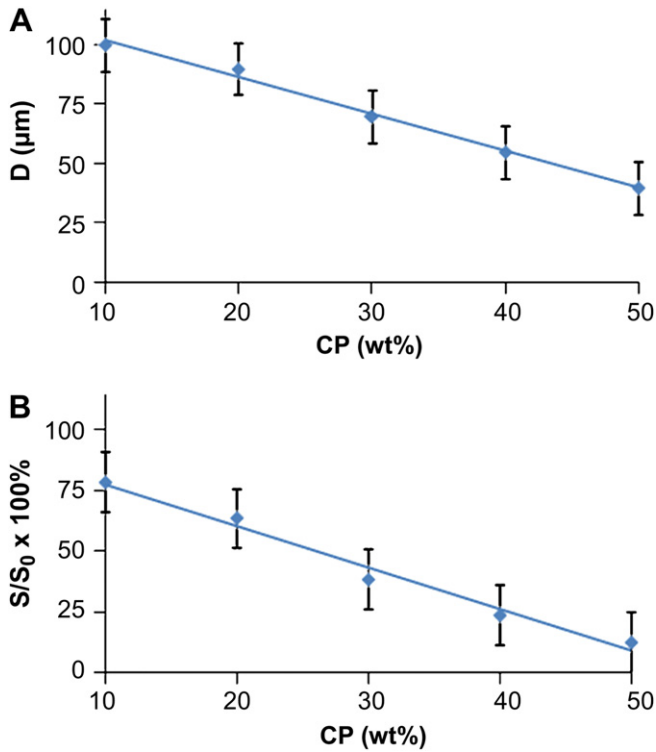


**Fig. 4.** Variation in the diameter,  $D_m$ , of the circular channel (A) and the resulting cross-sectional area of the circular channel (B), both plotted as a function of concentration of PDMS in hexanes ( $C_p$ ), from 10 to 50 wt.%, using 5 psi nitrogen pressure.

### 3.3. Modification of PDMS microchannels with constrictions

To explore the ability to modify the cross-sections of microchannels with complex geometries, the procedure described above

was tested on microchannels with a change in microchannel geometry. A  $100 \times 115 \mu\text{m}$  microchannel with a  $60 \mu\text{m}$ -wide constriction (shown in Fig. 5A) was modified to transform its square cross-section into a circular cross-section. The bright field images of the microchannel prior to and after modification are shown in Fig. 5A and B, respectively, with the corresponding images of the cross-sections of the channel-at-large and in the constriction, shown in Fig. 5A', B' and Fig. 5A'', B'', respectively. The fluorescence optical microscopy image of the cylindrical microchannel with a constriction filled with an aqueous solution of rhodamine fluorescent dye is shown in Fig. 5C. Following the modification, both the cross-sections of the channel-at-large and that of the constriction became circular, however the geometry of the channel was preserved. The constriction diameter became  $57 \pm 5 \mu\text{m}$ , whereas the diameter of the modified microchannel was  $99 \pm 3 \mu\text{m}$  upstream of the constriction and  $97 \pm 3 \mu\text{m}$  downstream of the constriction. We note that comparison of Fig. 5A'' and B'' indicates that the method described in the present work can be used to create microchannels with a symmetric circular opening from the channels with asymmetric cross-sections.

### 4. Endothelialization of circular PDMS microchannels

PDMS microchannels with a circular cross-section were coated with adherent endothelial cells to mimic a small diameter blood vessel. To ensure that cells were attached to the entire circumference of the cross-section of the microchannel, the microfluidic device was rotated during 4 h-long cell seeding, as described in the Experimental section. Fig. 6A and B shows phase contrast and fluorescent images of the cells attached to the surface of the microchannels. Adhesion of PAECs around the entire microchannel circumference was confirmed by sectioning the channel and observing PAEC nuclei by fluorescent microscopy (Fig. 6C).

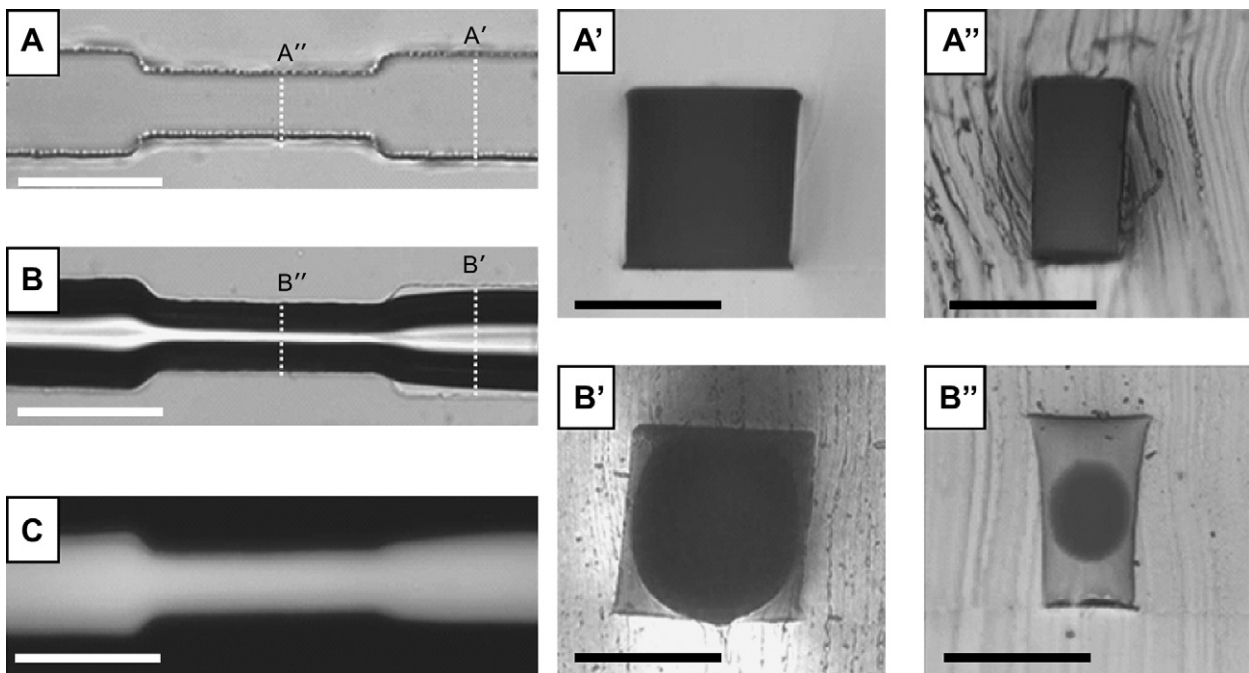


**Fig. 5.** (A) An unmodified microchannel filled with air and its cross-sections in the channel-at-large (A') and in the constriction (A''). (B) A modified microchannel filled with air and its cross-sections in the channel-at-large (B') and in the constriction (B''). Dashed lined indicate where the channel was cut to get cross-section images. A modified microchannel filled with rhodamine solution and captured using fluorescence mode (C). The scale bar in A, B, and C is  $150 \mu\text{m}$ . The scale bar in A', A'', B', and B'' is  $60 \mu\text{m}$ .

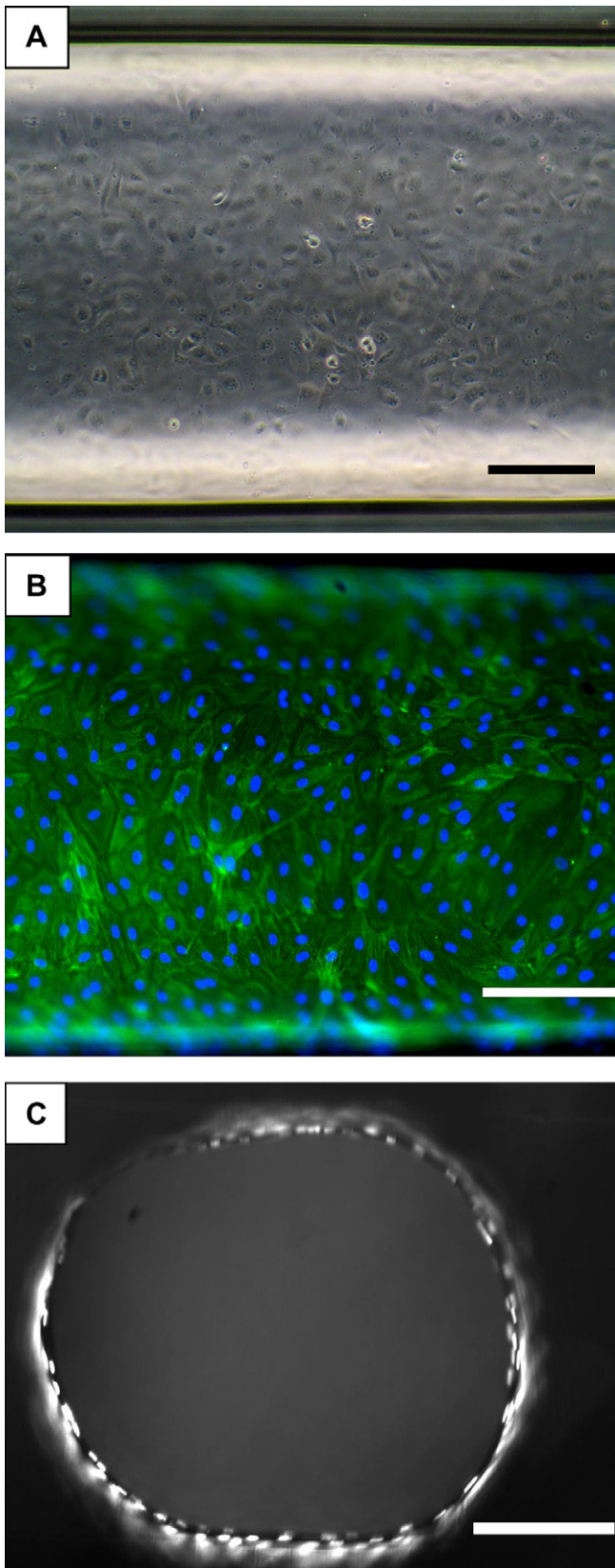


**Fig. 6.** (A) Phase contrast image of cells attached to circular channel wall. (B) Merged fluorescent image of filamentous F-actin (green) and nuclei (blue) of cells on channel wall. (C) Channel cross-section showing cell nuclei around the entire circumference. Scale bars are 200  $\mu\text{m}$ .

## 5. Conclusions

We have demonstrated a method for producing microfluidic channels mimicking a blood vessel in the micro-cardiovascular system. We show that we can controllably generate microchannels with a circular cross-section, with the diameter controlled by the pressure of the  $\text{N}_2$  stream and the concentration of silicone oligomers in the solution introduced in the microchannel. The method is applicable for the modification of topographically patterned microchannels. The modified microchannels can be further modified with endothelial cells to better mimic *in vivo* systems for cell flow studies. In addition, we expect that the proposed method can be adapted to the solutions of biopolymers, which will gel around a template gas stream and form cylindrical cell scaffolds for creating artificial blood vessels *in vitro*.

## Acknowledgements

The authors thank NSERC Canada, CIHR Canada, the Heart and Stroke Foundation of Ontario, and the Canada Research Chairs program for financial support of this work. After this paper was accepted, we learned that a similar approach to the fabrication of a circular cross-section PDMS microfluidics system was reported by Abdelgawad et al., [21].

## Appendix

Figures with essential color discrimination. Figs. 1, 3, 4 and 6 in this article are difficult to interpret in black and white. The full color images can be found in the on-line version, at doi:10.1016/j.biomaterials.2010.01.082.

## References

- [1] Gabriele S, Benoliel A-M, Bongrand P, Theodoly O. Microfluidic modeling of circular leukocyte deformation. *IFMBE Proc* 2008;22:1959–62.
- [2] Zhang X, Jones P, Haswell SJ. Attachment and detachment of living cells on modified microchannel surfaces in a microfluidic-based lab-on-a-chip system. *Chem Eng J* 2008;135S:S82–8.
- [3] Tsukada K, Sekizuka E, Oshio C, Minamitani H. Direct measurement of erythrocyte deformability in diabetes mellitus with a transparent microchannel capillary model and high-speed video camera system. *Microvasc Res* 2001;61:231–9.
- [4] Shelby JP, White J, Ganesan K, Rathod PK, Chiu DT. A microfluidic model for single-cell capillary obstruction by *Plasmodium falciparum*-infected erythrocytes. *Proc Nat Acad Sci* 2001;100:14618–22.
- [5] Yap B, Kamm RD. Mechanical deformation of neutrophils into narrow channels induces pseudopod projection and changes in biomechanical properties. *J Appl Physiol* 2005;98:1930–9.
- [6] Abkarian M, Faivre M, Stone HA. High-speed microfluidic differential manometer for cellular-scale hydrodynamics. *Proc Nat Acad Sci* 2006;103:538–42.
- [7] Higgins JM, Eddington DT, Bhatia SN, Mahadevan L. Sickle cell vasoocclusion and rescue in a microfluidic device. *Proc Nat Acad Sci* 2007;104:20496–9.
- [8] Shao JY, Hochmuth RM. The resistance to flow of individual human neutrophils in glass capillary tubes with diameters between 4.65 and 7.75 microns. *Microcirculation* 1997;4:61–74.
- [9] Lima R, Wada S, Tanaka S, Takeda M, Tsubota K-I, Ishikawa T, et al. Velocity measurements of blood flow in a rectangular PDMS microchannel assessed by confocal micro-PIV system. *World congress on medical physics and biomedical engineering*. Berlin Heidelberg: Springer; 2006. pp. 283–286.
- [10] Perry H, Greiner C, Georgakoudi I, Cronin-Golomb M, Omenetto FG. Simple fabrication technique for rapid prototyping of seamless cylindrical microchannels in a polymer substrate. *Rev Sci Instrum* 2007;78:044302.
- [11] Lima R, Wada S, Tanaka S, Takeda M, Ishikawa T, Tsubota K-I, et al. *In vitro* blood flow in a rectangular PDMS microchannel. *Biomed Microdevices* 2008;10:153–67.
- [12] Xia Y, Whitesides GM. Soft lithography. *Annu Rev Mater Sci* 1998;28:153–84.
- [13] Pries A, Secomb T, Gessner T, Sperandio M, Gross J, Gaetgens P. Resistance to blood flow in microvessels *in vivo*. *Circ Res* 1994;75:904–19.
- [14] Suzuki Y, Tateishi N, Soutani M, Maeda N. Deformation of erythrocytes in microvessels and glass capillaries: effects of erythrocyte deformability. *Microcirculation* 1996;3:49–57.

- [15] Stadnik D, Chudy M, Brzozka Z, Dybko A. Spectrometric analysis using PDMS microfluidic detectors. *Bull Pol Acad Sci* 2005;53:163–5.
- [16] Jia YF, Jiang JH, Ma XD, Li Y, Huang HM, Cai KB, et al. PDMS microchannel fabrication technology based on microwire-molding. *Chin Sci Bull* 2008;53:3928–36.
- [17] Dahlin AP, Bergstrom SK, Andren PE, Markides KE, Bergquist J. Poly-(dimethylsiloxane)-based microchip for two-dimensional solid-phase extraction-capillary electrophoresis with an integrated electrospray emitter tip. *Anal Chem* 2005;77:5356–63.
- [18] Verma MKS, Mujumder A, Ghatak A. Embedded template-assisted fabrication of complex microchannels in PDMS and design of a microfluidic adhesive. *Langmuir* 2006;22:10291–5.
- [19] Abate AR, Lee D, Do T, Holtz C, Weitz DA. Glass coating for PDMS microfluidic channels by sol–gel methods. *Lab Chip* 2008;8:516–8.
- [20] Lee K, Kim C, Shin KS, Lee JW, Ju B-K, Kim TS, et al. Fabrication of round channels using the surface tension of PDMS and its application to a 3D serpentine mixer. *J Micromech Microeng* 2007;17:1533–41.
- [21] Abdelgawad M, Wu C, Chien WY, Sun Y. Fast, simple fabrication of circular microchannels in polydimethylsiloxane (PDMS). Paper presented at the 23rd IEEE International Conference on MEMS; 2010. Piscataway, NJ.
- [22] Zulfikar MA, Mohammad AW, Kadhum AA, Hilar N. Synthesis and characterization of poly(methyl methacrylate)/SiO<sub>2</sub> hybrid membrane. *Mater Sci Eng A* 2007;452–3:422–6.
- [23] Fiddes LK, Chan HKC, Wyss K, Simmons CA, Kumacheva E, Wheeler AR. Augmenting microgel flow via receptor–ligand binding in the constrained geometries of microchannels. *Lab Chip* 2009;9:286–90.
- [24] Fiddes LK, Young EW, Kumacheva E, Wheeler AR. Flow of microgel capsules through topographically patterned microchannels. *Lab Chip* 2007;7:863–7.
- [25] Farcas MA, Rouleau L, Fraser R, Leask RL. The development of 3-D, *in vitro*, endothelial culture models for the study of coronary artery disease. *Biomed Eng* 2009;8:1–11.
- [26] Humphry KJ, Ajdari A, Fernandez-Nieves A, Stone HA, Weitz DA. Suppression of instabilities in multiphase flow by geometric confinement. *Phys Rev E* 2009;79:0563101–5.